Simulation of fully coupled thermomechanical analysis of connecting rod. Engine type F4L912

REDOUANE ZELLAGUI[1*], LEILA KHAMMAR[2], AHMED BELLAOUAR[3]

[1]Transportation Engineering and Environment Laboratory,
Mentouri University, Constantine 1,
ALGERIA
[2]Mechanical Laboratory,
Mentouri University, Constantine 1,
ALGERIA
[3]Transportation Engineering and Environment Laboratory,
Mentouri University, Constantine 1,
ALGERIA

Abstract: This study is the thermo mechanical behavior model of connecting rod for an engine type F4L912. It aims to determine the optimum operating conditions under variable mechanical and thermal loads.
The two cases are considered tensile loading and compression of the connecting rod. The results obtained stress state, deformation and thermal fields, allow the establishment of a predictive model of areas heavily used and hence improve the design parameters of connecting rods including dimensioning phase. The numerical method used is the finite element as it is implemented in ANSYS software. The nodal solution provides the ability to accurate and locates the coordinates of the elements that are causing some damages to the connecting rod.

Keywords: Connecting rod, Thermomechnical, Thermal strain, small end, big end, numerical method.

1 Introduction

The connecting rods are organs of internal combustion engine bodies that support mechanical and thermal stress are very important. Our approach consists of modelling the thermo mechanical behaviour of the connecting rod, whose purpose is to show the different states of stress and strain that are responsible for the different degradations. In order to achieve this work, we considered a connecting rod of an engine type F4L912. Numerical modeling has become an essential tool for improving the design of machine elements. Improving the performance of a connecting rod of an engine requires a through knowledge of operating conditions and loading. The connecting rod is a mechanical part connecting two links of moving axes and allowing the transmission's force. It is associated with the crank in the crank-connecting rod system that allows the conversion of a rotational movement continues reciprocating rotation or translation. We tried to determinate the temperature field, stress and strain along the length of connecting rod.

The approach is to determine the stress field according to a thermo mechanical loading to predict the critical areas or regions. Figure 1 shows the damaged portion of the connecting rod removed from the site following an accident caused mainly by a sudden failure problem.
A literature review paper focusing on the technique of modelling of thermo mechanical in the material of an engine connecting rod under regular loading was developed by [1] In 2004 Adila Afzel make a comparison between the different cases of fatigue behaviour of forged steel and metal powders. The elastic finite element analyses were performed to calculate the concentrations of stresses, stress states, and strains. The SN approach was used to perform fatigue life predictions and compare it with

experimental results, [2] Mansour Rasekh, Mohammad Aseda Reza, Ali Jafari, They are studied the analysis of the loads exerted on the different parts of connecting rod (small end and big end) by an experimental method. [3] P. Brabec, P. Kefurt, C. Scholz, R. Voženílek. This study based on the calculation of the resistance and a distortion characteristics of an engine at the stop point of connecting rod. The finite element method has been used in the resolution of force and distortion problems. [4] Roman Celin, Boris Arzen ek, Dimitrij Kmeti, The connecting rod converts the alternative motion of the piston into the rotational movement of the crankshaft. During service (about 2 years of service), the connecting rods are exposed to various cyclic loads which cause the fatigue. [5] Sergio Baragetti and Simone Mori 2006. The analytical calculations on the connecting rod are very important for determining the forces of the gases and the inertia. In their studies were making a comparison between the new analytical method that is to be studied in this work and the old method. [6] The research group Fareham and Yoshitane and Hikari make an experimental study on the crank connecting rod system of a NISSAN engine, they were determining the temperature distribution on all elements (the piston, the connecting rod and the crankshaft) by a Thermocouple posed in the interest areas.

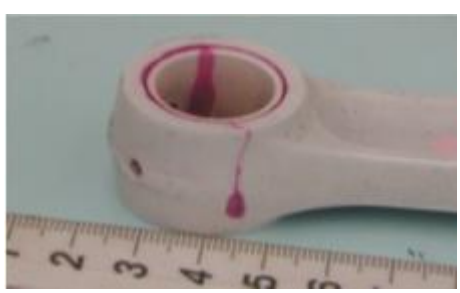

Fig. 1. Connecting rod damaged

To determine the total mass of the connecting rod, we propose a different method (Figure 2), which can give more accurate results with one model instead of two.

The connecting rod is divided into three parts; both ends and the central part. The central part remains as it is a rod with linear variable section and the both ends are modelled by two mass [6].

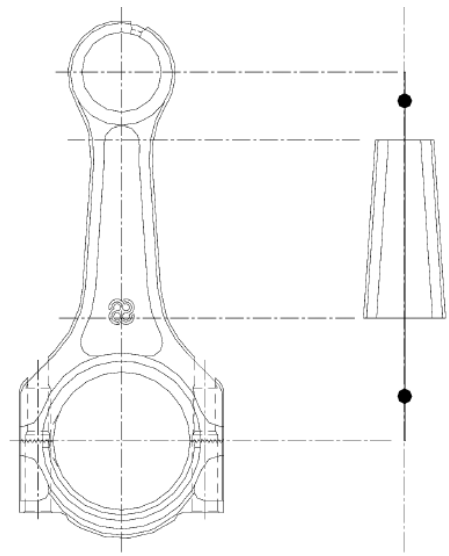

Fig. 2. Calculating the connecting rod mass method [6]

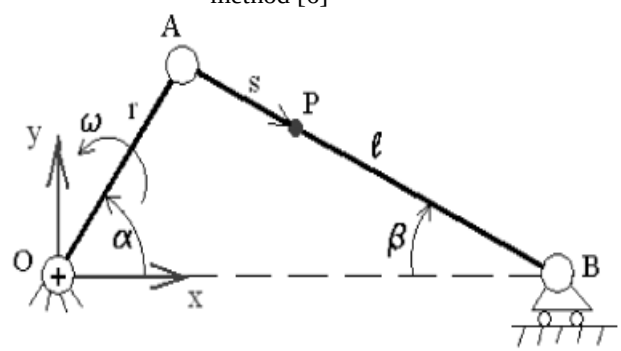

Fig. 3. Crank connecting rod system.

Figure 3 shows a global model of crank connecting rod system. From this figure we can determine the position and speed and acceleration of any point over the entire length of the connecting rod.

$$\begin{cases} Xp = r\cos\propto + s\cos\beta \\ Yp = r\sin\propto - s\ \sin\beta \end{cases} \quad (1)$$

We know that:

$$\cos\beta = \sqrt{1-\delta^2\ sin^2\alpha}$$

Where $\delta = \frac{r}{l}$

And:

$$\dot{\alpha} = \omega = \cos t\ :$$

$$\begin{cases} \dot{x}_p = -\omega\left(r\sin\alpha + s\frac{\lambda^2\ \sin 2\alpha}{2\sqrt{1-\delta^2\ sin^2\alpha}}\right) \\ \dot{y}_p = \omega(r-\delta s)\cos\alpha \end{cases} \quad (2)$$

Now, we need to determine the different loads applied on the connecting rod.

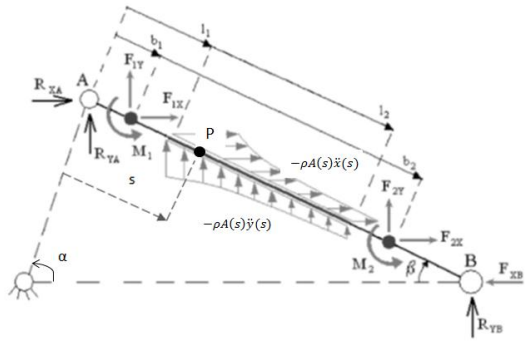

Fig. 4. Representation of the loads applied on the connecting rod [6]

$$\begin{cases} \sum F_x = 0: \; R_{XA} + F_{1X} + F_{2X} - F_{XB} \\ \quad - \int_{l_1}^{l_2} (\rho A(s)\ddot{x}(s))ds = 0 \\ \sum F_y = 0: \; R_{yA} + F_{1y} + F_{2y} - F_{yB} \\ \quad - \int_{l_1}^{l_2} (\rho A(s)\ddot{y}(s))ds = 0 \end{cases} \quad (3)$$

(III.7)

$$\sum M_A = 0: \left(F_{1y}b_1 + F_{2Y}b_2 + R_{YB}l - \int_{l_1}^{l_2} \rho A\ddot{x}s \, ds\right)\cos\beta + M_1 + M_2 + \left(F_{1x}b_1 + F_{2x}b_2 + R_{xB}l - \int_{l_1}^{l_2} \rho A\ddot{y}s \, ds\right)\sin\beta = 0 \quad (4)$$

Where:

$$I_1 = \int_{l_1}^{l_2} \rho A(s)\ddot{x}(s)ds$$
$$I_2 = \int_{l_1}^{l_2} (\rho A(s)\ddot{x}(s))sds$$
$$I_3 = \int_{l_1}^{l_2} \rho A(s)\ddot{y}(s)ds$$
$$I_4 = \int_{l_1}^{l_2} (\rho A(s)\ddot{y}(s))sds$$

$$\begin{cases} R_{XA} = I_1 - F_{1X} - F_{2x} + F_{xB} \\ R_{yA} = I_2 - F_{1y} - F_{2y} + F_{yB} \\ R_{YB} = \frac{1}{l}\left[\frac{M_1+M_2}{\cos\beta} - (F_{1x}b_1 + F_{2x}b_2 - F_{XB}l)\right] \\ \qquad \operatorname{tg}\beta + I_4 - F_{1y}b_1 - F_{2Y}b_2 \end{cases} \quad (5)$$

2. Boundary Conditions

2.1 The boundary conditions of mechanical loading

According to [3] we found that in terms of service connection from experience, the load distribution on the small end is applied to the upper half of the inner surface of a 180° angle cosine is in the form Figure 5.C'.

In the tensile case: the axle piston extends a cosine pressure on a 120° angle of the inner surface of the small end "figure"5.C. The same cases of load distribution are caused by the crankshaft on the big end of the connecting rod' figure 1A

In the press case, the axle piston compresses a uniform pressure on a 120° angle of the inner surface of the small end "figure"5.D. The same cases of load distribution are caused by the crankshaft on the big end of the connecting rod' figure 1B

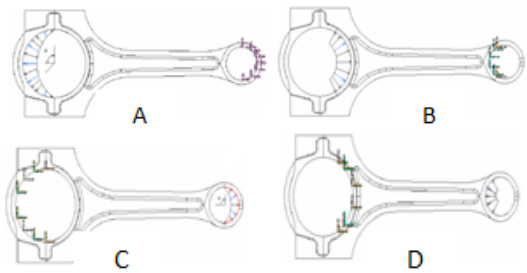

Fig. 5. Mechanical boundary conditions [1]

2.1 The boundary conditions of thermal loading

The boundary conditions of a body in space requested under thermal loading are of two types:

• Boundary condition of Neumann type: imposed derived. They require special treatment of the phases of problem solving (imposed flows ...).

• Boundary condition of Dirichlet type: imposed value. The value of the unknown is imposed (temperature).

3. Characteristics of Connecting Rod

All the characteristics of the connecting rod are given the temperature 25 (° C) and operating conditions are reported in Table 1. In addition, the material of connecting rod is 42CrMo4. According to references [6, 7], the limits of temperatures considered in our study is 150 (° C) in big end and 300 (° C) in small end.

Table 1. *Thermal and mechanical characteristics of the connecting rod [DIN SEW 310 (08/1992)]*

Température [°C]	Young Module E (GPa)	Thermal exponent (10^{-6})	thermal conductivity (W/m °C)	specific heat (J/kg °C)
20	212	11.5	45.1	461
200	199	12.7	44.1	499
300	192	13.2	41.9	517

3 CALCULATION OF THE LOAD EXERCISED ON THE CONNECTING ROD

The table 2 gives the values of pressure applied to big end and small end of connecting rod in a state of compression and tension.

Table 2. *The pressure applied to the connecting rod*

	Force applied to the big end	
	Tension	compression
The value of force (N)	58718	58718
The form of distribution	variable Distribution On 180	uniforme distribution On 120
Function of pressure	$p_0 = \frac{2p_t}{rt\pi}$	$p_0 = \frac{p_c}{rt\sqrt{3}}$
Value of pressure (MPa)	39.484	35.790
	Force applied to the small end	
	Tension	Compression
The value of force (N)	58718	58718
The form of distribution	variable Distribution On 180°	uniforme distribution On 120°
Function of pressure	$p_0 = \frac{2p_t}{rt\pi}$	$p_0 = \frac{p_c}{rt\sqrt{3}}$
Value of pressure (MPa)	61.131	55.411

4. Discussion and Results

4.1 Thermal Results

We know that the temperature at the small end is greater than that of the big end, hence our assumption for the thermal modeling 300 (° C) at small end and 150 (° C) at the big end. In our case, the boundary condition is imposed on the type of Dirichlet.

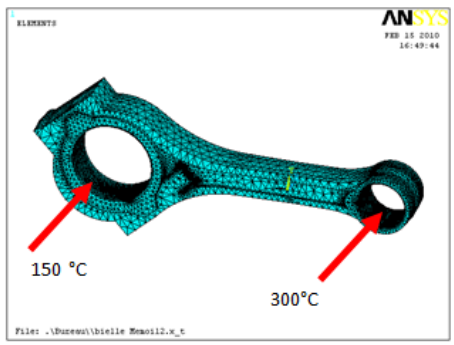

Fig. 6. Thermal boundary conditions

The Figure 7 shows the path followed to calculate the temperature profiles and thermal strain.

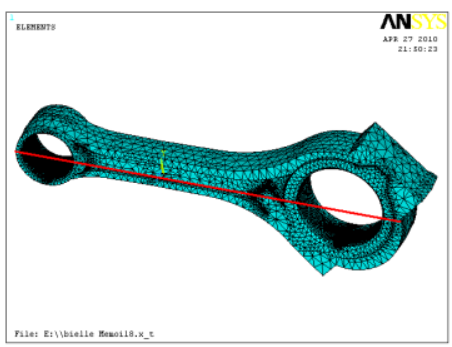

Fig. 7. Representation of the path used on the length of connecting rod

Figures 8 (a,b) show the temperature distribution of the thermal simulations carried out under ANSYS, with the representation of the distribution of the thermal gradients and the thermal flow along the axis of the connecting rod, and shows in more the discontinuity because of the shape of the singularities also the small and big end of the connecting rod.

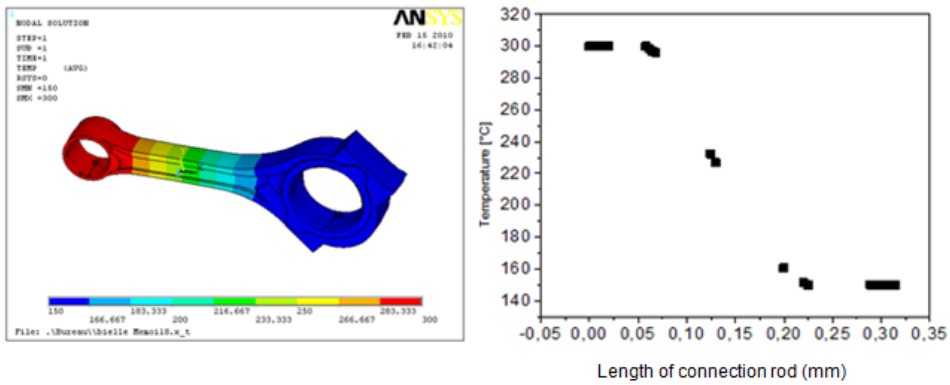

Fig. 8. Evolution of the temperature field

Figures 9 show that the thermal deformation of the connecting rod along their length is very important in the small end of a value of 0.00935 than in the big end, because the heat that transferred from the exhaust gases is very higher than the heat of contact between the big end and the crankshaft.

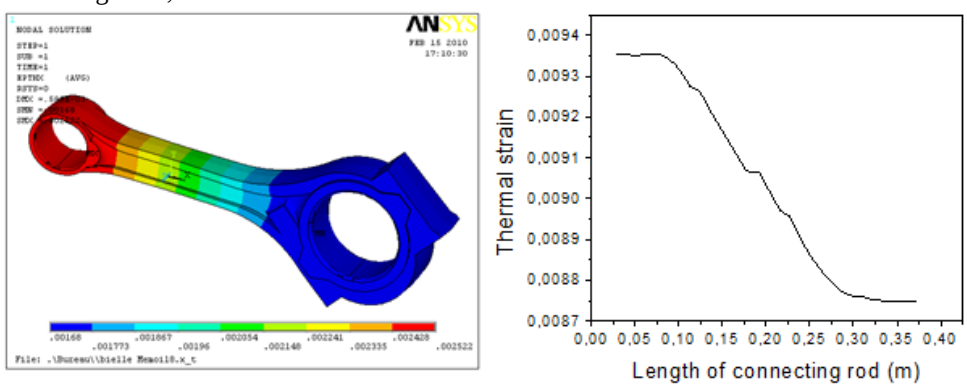

Fig. 9. Evolution of thermal strain

4.2 Mechanical and thermo mechanical results

We know that in any connecting rod there are three critical areas, which are shown in "Figure 10" The first area is located on the arm of connecting rod between nodes 15 and 9 and the second on the small end between nodes 88 and 120 and the third is the big end between nodes 116 and 118.

Fig. 10. Representation of the critical areas in connecting rod

The figures 11 shows that the stress range from 1.3E^8 (Pa) in the case A, 3.0E^8 (Pa) for C, 1.00 E^8 (Pa) in the case B and 2.4 E^8 (Pa) in D

According to the Von Mises relation, the fracture is located on the arm of the connecting rod which is consistent with reality.

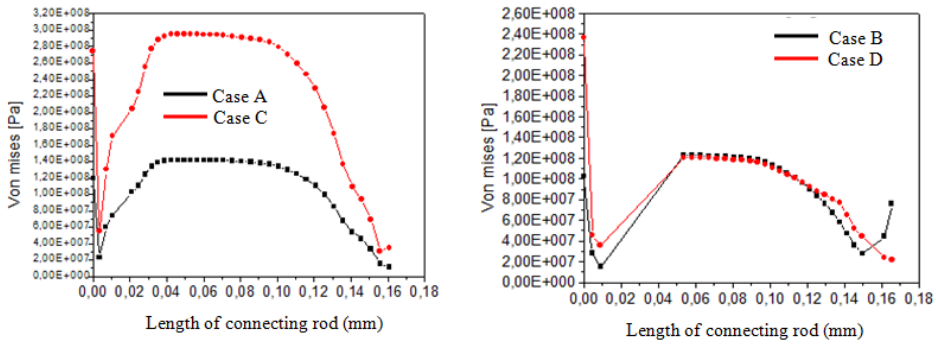

Fig. 11. Evolution of von Mises stress in region I

The figures'12 and 13' respectively show the evolution of the von Mises stress in regions II and III 'case of tension and compression, where one can notice that the area requested is the body of the connecting rod working in the traction and the area of cracking obtained in the small end.

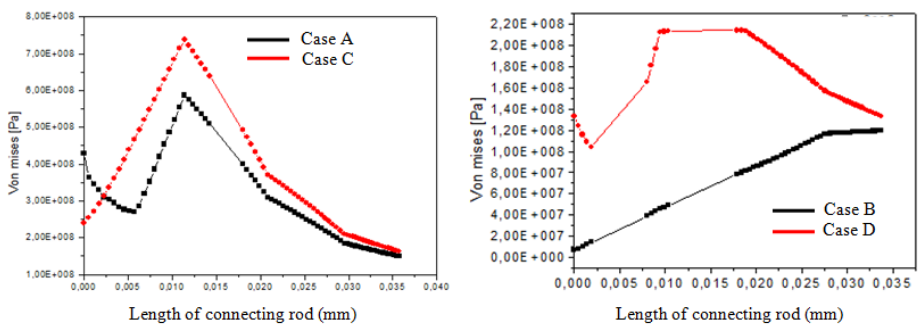

Fig. 12. Evolution of von Mises stress in region II

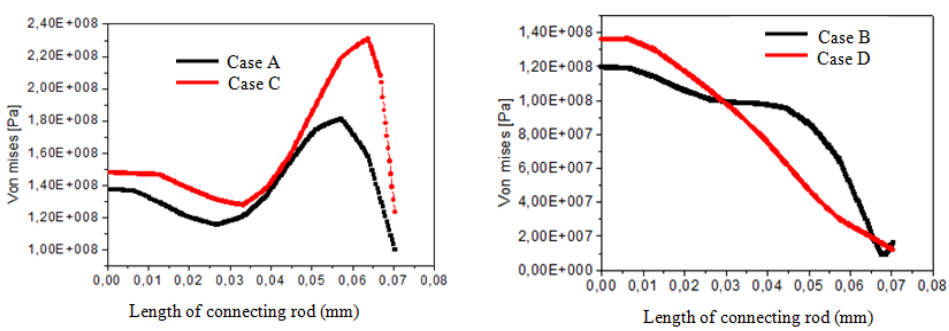

Fig. 13. Evolution of von Mises stress in region III

4.3 Influence of temperature on the mechanical strain

Because we are found that, the value of von mises stress is very big in the cases (C,D) than the cases (A,B), we consider that the worst case in tension and compression (third and fourth cases) with and without temperature. The histogram below shows clearly that the influence of temperature is significant on the thermo mechanical deformation. In our case the largest strain along the X axis with a value of 3.38 E-^{03} in the case of tension and along the Z axis with a value of 2.62 E^{-3} in the case of compression.

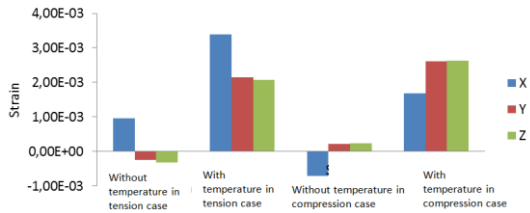

Histogram.1. Strains comparisons

The worst case in tensile and compression (third and fourth case) with and without temperature is considered.

Case A (tensile):

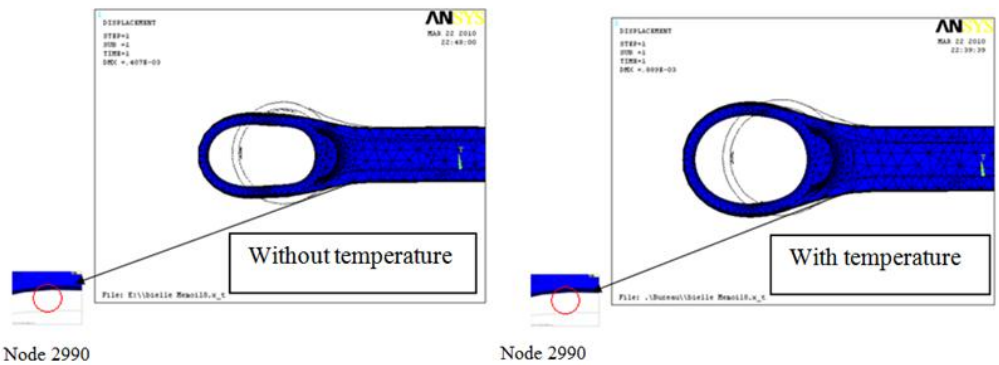

Fig. 14. Strain of small end with and without temperature

We take node 2990 and we determine are strains with and without temperature:

Table.3 *Evolution of strain*

	X	Y	Z
Without temperature	9,62E^{-04}	-2,56E^{-04}	-3,22E^{-04}
With temperature	3,38E^{-03}	2,14E^{-03}	2,08E^{-03}

The histogram below clearly shows that the influence of temperature is considerable on the thermo mechanical strain. In our case the greatest strain is along the X axis of a value of 3.38E^{-03}, in the case of tension of connecting rod.

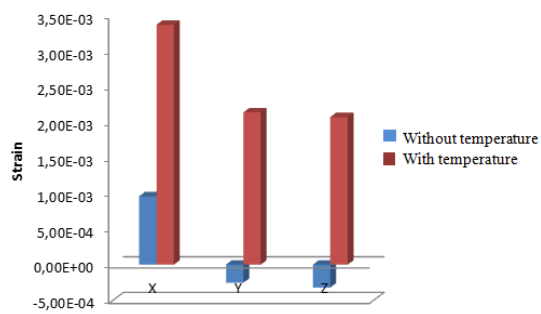

Histogram. 2. Comparison of strains in tensile cases

Case B (compression case):

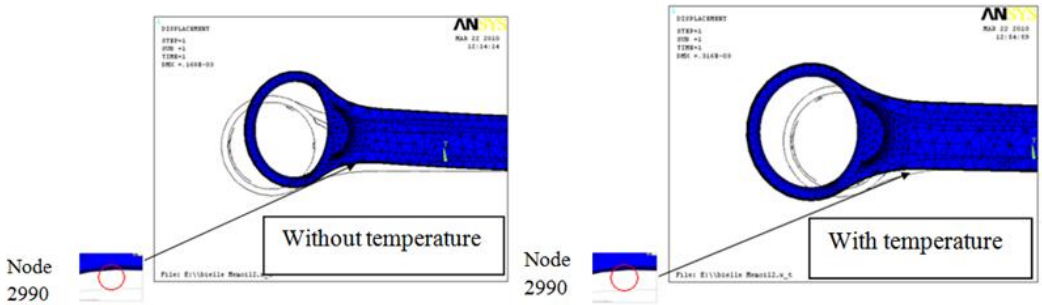

Fig. 15. Strain of small end with and without temperature

We take node 2990 and we determine the strains with and without temperature:

Table.4 *Evolution of strain.*

	X	Y	Z
without temperature	-7,20E^{-04}	2,08E^{-04}	2,29E^{-04}
with temperature	1,68E^{-03}	2,60E^{-03}	2,62E^{-03}

The histogram below clearly shows that the influence of temperature is considerable on the thermo mechanical deformation. In our case the largest deformation is along the Z axis of a value of 2.62 E^{-3}, in the case of pulling the connecting rod. The histogram 3 shows this comparison (state of buckling) which is compatible with the results of the reference [15].

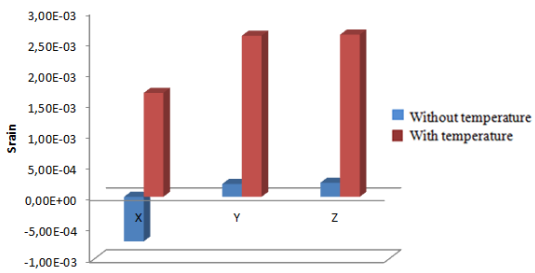

Histogram. 3. Comparison of strains in compression cases

5 Validation of Results

To validate our model of computation (presented in figure 17) we took an example of connecting rod studied by Adila Afzel [1] (presented in figure 16) giving the variation of the field of constraint of Von Mises. The same result was obtained on this geometric model modelled by Ansys, this is presented in figure 15.

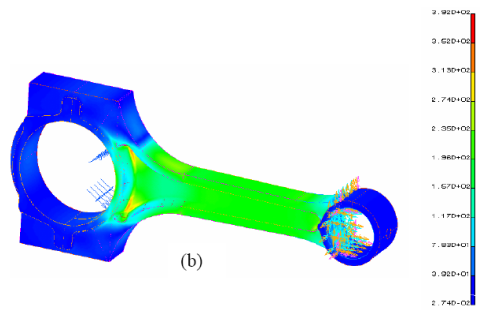

Fig. 16 a. Von mises study by the reference [1]

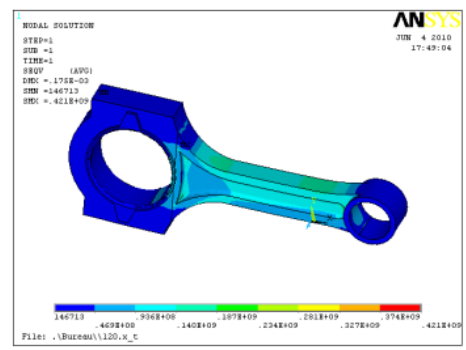

Fig. 17. Our calculation of Von mises

6. Conclusions

The connecting rods are organs of internal combustion engine that can withstand mechanical heat are important. Our approach is to model the thermo mechanical behavior of the connecting rod whose purpose is to show the different states of stresses and strains that are responsible for

different damages. To achieve this goal, it was considered a connecting rod of an engine type F4L912. The result thus found is consistent with the empirical results, which showed that the region of the small end is the seat of high stress concentration and consequently cracking and fatigue. We can say that the results found provide insight holding the connecting rod in different operating conditions and help to better geometric design of the connecting rod.

7 NOMENCLATURES

X_p, Y_p		coordinates of the center of gravity of connecting rod
r	[mm]	radius of crankshaft
l	[mm]	length of connecting rod
ω	[rads^{-1}]	rotation velocity
$\dot{x_p}, \dot{y_p}$	[ms^{-1}]	translation velocity
β	[rad]	rotation angle of connecting rod
α	[rad]	rotation angle of crankshaft
$A(s)$	[mm^2]	connecting rod section
F_x	[N]	load on the x axle
F_y	[N]	load on the y axle
R_{xA}	[N]	reactions between big end and crankshaft on the x axle
R_{yA}	[N]	reactions between big end and crankshaft on the y axle
R_{xB}	[N]	reactions between small end and piston axle on the x axle
R_{yB}	[N]	reactions between small end and piston axle on the y axle
M_1	[Nmm^{-1}]	rotation moment in the gravity centre of big end
M_2	[Nmm^{-1}]	rotation moment in the gravity centre of small end
$A(s)$	[mm^2]	connecting rod section
ρ	[Kgm^{-3}]	density
I_1,I_2,I_3,I_4	[Kgm^2]	inertia moments

References

[1] Adila, A. (2004). Le Comportement en Fatigue de L'acier Forgé et des Bielles de Poudres Métalliques, The University of Toledo

[2] Mansour, R. Mohammad, R. Ali, J. Kamran, KH. (2009). Obtaining Maximum Stresses in Different Parts of Tractor (Mf-285) Connecting Rods Using Finite Element Method.

[3] Vozenilek, R. Scholz,C. Brabec,P (2004). FEM Analyse of connecting rod.

[4] Celin, R. (2007). A metallographic examination of a fractured connecting rod.

[5] Sergio, B. Simone, M. (2006). A study on connecting rods for IC engines.

[6] Shoichi, F. Yoshitane, O. Hikari, S. (1966). Temperature Measurements of the Connecting Rod, Piston Pin and Crankpin Bearing of an Automobile Gasoline Engine.

[7] Zoumana, S. (2005). Etude du Couplage Thermomécanique dans la Propagation Dynamique de Fissure.

[8] Webster, D. Coffell, R. Alfaro, D. (1983). A Three Dimensional Finite Element Analysis of a High Speed Diesel Engine Connecting Rod.

[9] Yves, M. (2002). Couplage Thermomécanique et Approche non Entière de L'irréversibilité en Viscoélasticité.

[10] Aurelian, F. (2005) Modélisation numérique et expérimentale de la lubrification des paliers de moteur soumis à des conditions sévères de fonctionnement.

[11] Miloud, T. Mohamed, H. Patrick, M. (2001). Un modèle global de piston de moteur a combustion interne.

[12] Lothar, A. Exemple de la fabrication des bielles.

[13] Claudio, L. (2009). Amélioration des Techniques de Génération de maillages 3D des structures anatomiques humaines pour la Méthode des Éléments Finis.

[14] Ibrahim, G. (2006). The finite element method and applications in engineering using ansys.

[15] Sergio, B. Simone, M. (2006). A study on connecting rods for IC engines.